

# Self-ratcheting Stokes drops driven by oblique vibrations

Karin John\*

Laboratoire de Spectrométrie Physique UMR 5588, Université Joseph Fourier - Grenoble I, BP 87 - 38402 Saint-Martin-d'Hères, France

Uwe Thiele†

Department of Mathematical Sciences, Loughborough University, Loughborough, Leicestershire, LE11 3TU, UK

We develop and analyze a minimal hydrodynamic model in the overdamped limit to understand why a drop climbs a smooth homogeneous incline that is harmonically vibrated at an angle different from the substrate normal [Brunet, Eggers and Deegan, *Phys. Rev. Lett.* **99**, 144501 (2007)]. We find that the vibration component orthogonal to the substrate induces a nonlinear (anharmonic) response in the drop shape. This results in an asymmetric response of the drop to the parallel vibration and, in consequence, in the observed net motion. Beside establishing the basic mechanism, we identify scaling laws valid in a broad frequency range and a flow reversal at high frequencies.

PACS numbers: 68.15.+e, 47.20.Ma, 05.60.-k, 68.08.Bc

The concept of transport driven by an external ratchet potential dates back to Pierre Curie [1]. He states that a locally asymmetric but globally symmetric system may induce global transport if it is kept out of equilibrium. Practical realizations include colloidal particles that may move either through periodic asymmetric micropores when driven by an imposed oscillating pressure field [2] or they can be driven by a saw-tooth dielectric potential that is periodically switched on and off [3]. Many different variations of ratchet mechanisms are nowadays studied [4]. They are employed to transport or filter discrete objects [2, 3] or to induce macroscopic transport of a continuous phase in systems without a macroscopic gradient [5, 6, 7]. Most modelling effort is focused on the former, but first models do as well exist for the latter [8, 9].

An experiment that at first sight seems unrelated has recently shown that drops may climb an inclined homogeneous substrate if it is vibrated harmoniously in a vertical direction [10]. The experiment is quite remarkable, as previously it had only been shown that substrate vibrations can 'unlock' drops pinned by substrate heterogeneities and therefore facilitate directed motion of drops in a global gradient. In particular, they allow to overcome effects of contact angle hysteresis on non-ideal substrates with a global wettability gradient [11, 12]. A recent extension shows that drops can as well be driven by simultaneous vertical and horizontal substrate vibrations that are phase-shifted [13]. Several hypothesis have been put forward as to why the vibrations induce the drop motion. Contact angle hysteresis, nonlinear friction, anharmonicity of the vibrations, convective momentum transport are all mentioned as possible 'minimal ingredients' [10, 13, 14]. Anharmonic lateral vibrations with non-zero mean displacement are known to drive drop motion on horizontal substrates [15]. In general, several studies have addressed drops and free surface films on oscillating substrates since early work by Faraday, Kelvin and Rayleigh [16]. However, most consider fixed contact lines

[17, 18], purely inviscid flows [19, 20] or a high frequency limit [21]; and, most importantly, limit their study to vibrations either parallel or orthogonal to the substrate.

In the present Letter we analyze a minimal hydrodynamic model for the situation depicted in Fig. 1 and show which of the above mentioned ingredients are not necessary for the drop motion to occur. We derive a thin film evolution equa-

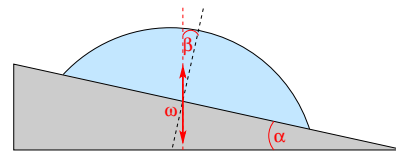


FIG. 1: (color online) Sketch of a drop on a vibrating (frequency  $\omega$ , vibration angle with the substrate normal  $\beta$ ) inclined substrate (inclination angle  $\alpha$ ).

tion in the overdamped limit, i.e., based on a pure Stokes flow (no convective momentum transport) for a drop on an ideally smooth homogeneous inclined substrate (no contact angle hysteresis). The obtained results show that harmonic vibrations are sufficient to drive a drop in a directed manner on a horizontal substrate [13] or as well up an incline [10].

Analysing the underlying mechanism we find that the component of the harmonic vibration that is orthogonal to the substrate induces a nonlinear (anharmonic) response in the drop shape. As the latter determines the strongly nonlinear drop mobility this results in an asymmetric response of the drop to the vibration component that is parallel to the substrate. The induced symmetry breaking between forward and backward motion during the different phases of the vibration results in the observed net motion of the drop. This phenomenon can be seen as a rocked self-ratcheting of the drop [4] as it is the drop itself that introduces the local time-reflection asymmetry in the response to the time-periodic driving of the sliding motion.

In the following we first present the model, then analyze it in the low frequency limit employing continuation techniques. Results for higher frequencies are obtained through numerical time integration. We use a long-wave approximation [22, 23]

\*Electronic address: kjohn@spectro.ujf-grenoble.fr

†Electronic address: u.thiele@lboro.ac.uk;  
URL: <http://www.uwethiele.de>

to describe the dynamics of a drop of liquid on an inclined substrate (inclination angle  $\alpha$ ) that is subject to harmonic vibrations (frequency  $\omega$ , at angle  $\beta$  to the substrate normal, see Fig. 1). We consider a two-dimensional (2d) drop as we do not expect any conceptual difference to the 3d case. The resulting evolution equation for the film thickness profile  $h(x, t)$  is

$$\partial_t h = \partial_x \left[ \frac{h^3}{3\eta} (\partial_x p - f) \right]. \quad (1)$$

The divergence of the flow on the r.h.s. is expressed as the product of a mobility and the sum of a pressure gradient  $\partial_x p$  and a lateral driving force  $f$ .  $\eta$  is the dynamic viscosity. The pressure

$$p = -\gamma \partial_{xx} h - \Pi(h) + \rho g h [1 + a(t)] \quad (2)$$

contains the curvature pressure  $-\gamma \partial_{xx} h$ , where  $\gamma$  denotes surface tension, the disjoining pressure  $\Pi(h)$  that incorporates wettability [22, 24] and the hydrostatic pressure  $\rho g h [1 + a(t)]$ , where the time dependence results from the vibration component normal to the substrate. The lateral force

$$f = \rho g [\alpha + \beta a(t)]. \quad (3)$$

contains a constant part (force down the incline) and a time-modulated part (vibration component parallel to the substrate). The function  $a(t) = a_0 \sin(\omega t)$  corresponds to the acceleration in units of  $g$ . The drop experiences a force of opposite sign, e.g., if the substrate is accelerated upwards and to the left the drop is flattened and pushed to the right. The partial wettability of the substrate is modelled through a precursor film model based on the disjoining pressure  $\Pi = (A/h^3 + B/h^6)/6\pi$ . It combines long-range destabilizing ( $A < 0$ ) and short-range stabilizing ( $B > 0$ ) van der Waals interactions [25].

Note, that consistency of the long-wave approach requires small free surface slopes as well as  $\alpha, |\beta| \ll 1$  [23]. However, it is known that equations like (1) often predict the correct qualitative behavior even for systems with larger contact angles [22]. In consequence, we expect the here obtained results to hold qualitatively as well for larger  $\beta$ .

To nondimensionalize we introduce the scales  $t_0 = 3\gamma\eta/h_0\kappa^2$ ,  $x_0 = \sqrt{\gamma h_0/\kappa}$ , and  $h_0 = (B/A)^{1/3}$  for  $t$ ,  $x$ , and  $h$ , respectively, where  $\kappa = A/6\pi h_0^3$ . The resulting dimensionless equations correspond to Eqs. (1)-(3) with  $3\eta = \gamma = B = 1$  and  $A = -1$ . The dimensionless modulated hydrostatic pressure and lateral force are  $p_h = Gh [1 + a(t)]$  and  $f = G(\alpha + \beta a(t))$  with  $G = \rho g h_0/\kappa$ . The vibration period  $T = 2\pi/\omega$  is given in units of  $t_0$ . The fixed drop volume  $V = L(\bar{h} - h_p)$  is determined by the domain size  $L$ , the mean film thickness  $\bar{h}$  and the precursor film thickness  $h_p = 1$ . The resulting transport along the substrate is measured after all transients have decayed and the vibration-induced shape changes of the drop are completely periodic in time. We quantify the transport by the mean drop velocity  $\langle v \rangle = \Delta x/T$  where  $\Delta x$  denotes the distance the drop moves within one period  $T$ .

Fig. 2 illustrates the typical behaviour of a drop during one vibration cycle. One notices forward/backward lateral motion

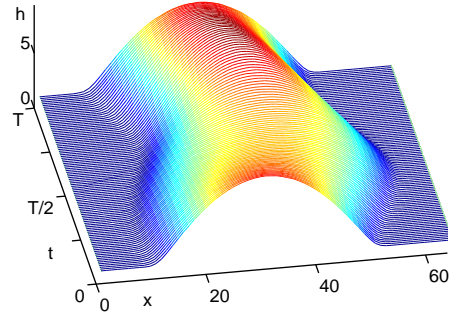


FIG. 2: (color online) Space-time plot illustrating the evolution of the profile of a drop on a obliquely vibrated substrate during one vibration period. Each cycle results in the net motion of the drop to the left. The starting time is well after initial transients have decayed. Note that only part of the domain  $L$  is shown. Parameters are  $V = 192$ ,  $G = 0.001$ ,  $\beta = 0.1$ ,  $\alpha = 0$ ,  $T = 400$ ,  $L = 128$ ,  $a_0 = 10$ .

and small but significant changes of shape. In particular, the drop becomes flatter and broader during the first part of the cycle when its center of mass moves to the right ( $t < T/2$ , substrate acceleration is upward and to the left). In the second half of the cycle the drop becomes again higher and less wide while it moves to the left ( $t > T/2$ , substrate acceleration is downward and to the right). After one period the drop has moved a net distance to the left. In the course of one period, the orthogonal component of the oblique vibration modulates the hydrostatic pressure and causes a nonlinear response in the drop shape. That in turn determines the strongly nonlinear drop mobility [ $h^3/3\eta$  in Eq. (1)] and therefore induces an anharmonic response of the drop to the harmonic parallel vibration component that results in the observed net motion. Note, that a harmonic back and forth forcing alone results in zero net motion.

First, we consider a slowly vibrating substrate, i.e. the typical timescale of the intrinsic drop dynamics  $t_0$  is small compared to the vibration period  $T$ . In this low frequency limit the drop moves in a quasi-stationary manner, i.e., its shape and velocity at each instant during the vibration cycle are those of a stationary moving drop at the corresponding acceleration. The resulting family of moving drop solutions is parametrized by  $a(t)$  and can be obtained using continuation techniques [26, 27, 28]. Averaging stationary drop velocities  $v(a(t))$  over one vibration period gives the low frequency limit of  $\langle v \rangle$ .

Figs. 3 (a) and (b) show profiles of stationary moving drops and their velocities at various phases of the cycle on a horizontal substrate. As observed already in Fig. 2, during the first [second] half cycle the drop is compressed [decompressed] and slides to the right [left]. Fig. 4 shows the relationship between acceleration  $a$  and the drop velocity  $v$ . The difference between the two respective curves for positive and negative acceleration is a measure of the anharmonic response of the drop. The mean velocity in the low frequency limit then corresponds to twice the weighted area of the shaded region in Fig. 4(a) when taken from  $a = 0$  to  $a = a_0$ . A numerical analysis gives  $\langle v \rangle \sim a_0^2$ ,  $\langle v \rangle \sim \beta$  and  $\langle v \rangle \sim V^{1.67}$ . Note

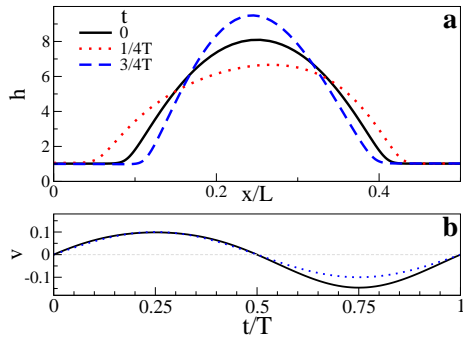


FIG. 3: (color online) Shown are (a) several drop shapes and (b) the velocity during one vibration cycle for an obliquely vibrated horizontal substrate in the low frequency limit. For the used  $\beta = 0.3$  the drop moves with  $\bar{v} \approx -0.01$ , i.e., to the left. The blue dotted line in (b) indicates a harmonic variation of zero net flow. Remaining parameters are as in Fig. 2.

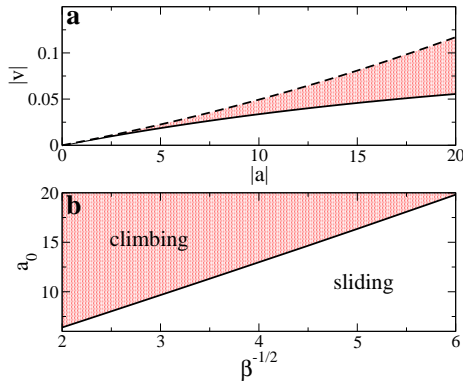


FIG. 4: (color online) (a) Mean drop velocity depending on the acceleration  $a$  for a horizontal substrate. The solid (dashed) line indicates  $a > 0, v > 0$  ( $a < 0, v < 0$ ). (b) Phase diagram indicating the regions of sliding and climbing drops in the  $a_0 - \beta^{-1/2}$ -plane for a substrate inclination of  $\alpha = 0.1$ . The results for (a) and (b) are in the low frequency limit with the remaining parameters as in Fig. 2.

that for positive  $\beta$  in the present limit net transport is always directed to the left.

From the transport properties on a horizontal substrate it is obvious, that such a vibration-caused motion can overcome a further external driving and, e.g., move a drop up an incline or against a wettability gradient, as long as the product  $\beta a_0^2$  is larger than a critical value. This is confirmed by the phase diagram Fig. 4(b), as there the straight line  $a_0 \sim \sqrt{v_0/\beta}$  separates climbing from sliding drops, where  $v_0$  is the drop velocity for the given substrate inclination without any vibration. Note that the case  $\beta = \alpha$ , i.e., a vibration vertical in the laboratory frame, is by no means special: uphill motion is generated above a finite threshold acceleration. However, in the limit  $\beta \rightarrow 0$ , i.e., for a vibration normal to the substrate, the threshold acceleration becomes infinite and the net transport is zero.

For practical purposes, e.g., for microfluidic applications, drops need to be transported in a limited time, i.e., the behaviour at sufficiently large frequencies has to be understood.

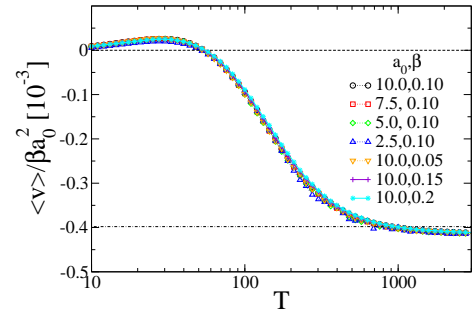


FIG. 5: (color online) Master curve for the scaled mean velocity  $\langle v \rangle / \beta a_0^2$  as a function of the vibration period  $T$  for sets  $(a_0, \beta)$  as given in the legend. The horizontal dashed line indicates the result in the low frequency limit. Remaining parameters are as in Fig. 2.

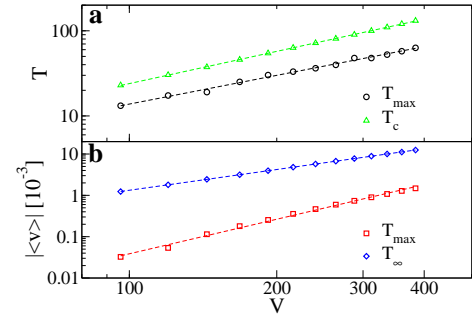


FIG. 6: (color online) Dependence of transport on drop volume: (a) shows the special vibration periods  $T_{\max} \sim V^{1.12 \pm 0.03}$  and  $T_c \sim V^{1.26}$ , as detailed in the text; (b) gives the absolute value of the mean velocities  $\langle v \rangle_{\max} \sim V^{2.78 \pm 0.06}$  at period  $T_{\max}$  and in the low frequency regime ( $T_{\infty}$ ). Remaining parameters are as in Fig. 2.

We study that regime employing an adaptive time-step 4th order Runge-Kutta method and prevent numerical instabilities by a switching upwind differencing for the driving term. The above deduced scaling  $\langle v \rangle \sim a_0^2 \beta$  still holds in a large frequency range, illustrated in Fig. 5 by collapsing dependencies of mean velocity on vibration period for various sets  $(a_0, \beta)$  onto a single master curve. A second interesting feature is the observed reversal of net transport at a small critical period  $T_c \approx 55$  that results in a (small) positive mean velocity even for a horizontal substrate ( $\alpha = 0$  as in Fig. 5). The reversed flow is strongest at  $T_{\max} \approx T_c/2 \approx 27$ , but always about one order of magnitude smaller than the transport to the left in the low frequency regime. Note that in agreement with the first observation  $T_c$  and  $T_{\max}$  are nearly independent of  $a_0$  and  $\beta$ . They do, however, depend on drop volume (see Fig. 6) indicating that the flow reversal might be triggered when the vibration frequency becomes larger than an eigen frequency of the drop, i.e., for larger imposed frequencies the response of the drop becomes delayed and phase-shifted w.r.t. the forcing. This is corroborated by an inspection of drop profiles over the course of a cycle (not shown). This result is similar to the dependence of the direction of net motion on the phase-shift between vertical and horizontal vibration observed in [13].

Finally, Fig. 7 presents a phase diagram that shows the

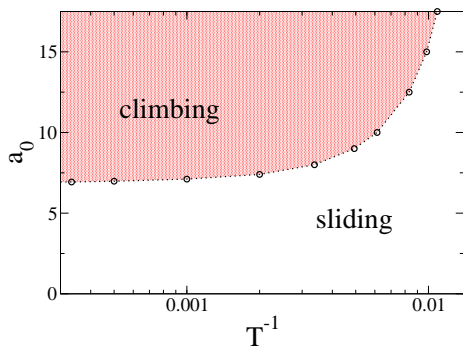


FIG. 7: (color online) Phase diagram of sliding and climbing drops in the  $(a_0, 1/T)$  plane for an obliquely vibrated inclined substrate. Beside  $\alpha = 0.05$  parameters are as in Fig. 2.

influence of the vibration period and peak acceleration on the transport direction for fixed substrate inclination angle  $\alpha = 0.05$ . The critical acceleration  $a_c(T^{-1})$  separating sliding and climbing drops approaches a constant at small frequencies and diverges at finite  $T_c^{-1}$ . As we do not model any effects of non-ideal substrates (contact angle hysteresis, contact line pinning) our phase diagram differs in two aspects from the experimental one [10]: (i) we find a monotonic decrease of  $a_c$  with decreasing frequency ( $T^{-1}$ ) whereas [10] finds evidence for a small increase at small  $T^{-1}$ ; and (ii) here drops always slide down below  $a_c$  whereas in the experiments one finds instead a transition between static and climbing drops at large  $T^{-1}$ .

To conclude, we have proposed and analyzed a minimal hydrodynamic model for the experimentally observed drop motion that is driven by harmonic oblique substrate vibrations

[10]. Our analysis has ruled out convective momentum transport, anharmonicity of vibrations and contact angle hysteresis as necessary for the motion. The mechanism that moves drops on a horizontal substrate or even up an incline is based on a nonlinear response of the drop shape to the normal vibration component. This breaks the back-forth symmetry of the response of the drop to lateral oscillations and therefore causes a net motion. The found mechanism is in line with the hypothesis put forward in [10] based on a mechanical analogue that a breaking of the front-back symmetry due to a nonlinear friction law is sufficient to induce transport. Here, we have identified the strongly shape-dependent nonlinear mobility in Eq. (1) as the relevant hydrodynamic 'nonlinear friction'. Beside establishing the basic mechanism, our analysis has revealed several interesting features that should be investigated in future experiments. In particular, we have identified a number of scaling laws valid in a broad frequency range and found a flow reversal at high frequencies.

We have argued that the phenomenon can be seen as a self-ratcheting of the drop as its shape changes are instrumental in producing local time-reflection asymmetries. Comparing Eq. (1) with Fokker-Planck descriptions for ratchet systems of interacting particles [4, 29] one may further the analogy by noting that (i) the lateral vibration component corresponds to an imposed rocking, (ii) the orthogonal vibration component corresponds to an imposed temporal temperature modulation, (iii) the role of the spatial asymmetry in the ratchet potential is here taken by non-linear couplings due to strongly nonlinear prefactors of the diffusion (2nd order) and the transport (1st order), (iv) our surface tension term is analogous to a mean field expansion of the distribution function up to second order.

- 
- [1] P. Curie, *J. Phys. (Paris)* **III**, 383 (1894).  
 [2] S. Matthias and F. Müller, *Nature* **424**, 53 (2003).  
 [3] J. Rousselet, L. Salomé, A. Ajdari, and J. Prost, *Nature* **370**, 446 (1994).  
 [4] P. Hänggi and F. Marchesoni, *Rev. Mod. Phys.* **81**, 387 (2009).  
 [5] A. D. Stroock, R. F. Ismagilov, H. A. Stone, and G. M. Whitesides, *Langmuir* **19**, 4358 (2003).  
 [6] D. Quéré and A. Ajdari, *Nat. Mater.* **5**, 429 (2006).  
 [7] A. Buguin, L. Talini, and P. Silberzan, *Appl. Phys. A - Mater. Sci. Process.* **75**, 207 (2002).  
 [8] A. Ajdari, *Phys. Rev. E* **61**, R45 (2000).  
 [9] K. John and U. Thiele, *Appl. Phys. Lett.* **90**, 264102 (2007).  
 [10] P. Brunet, J. Eggers, and R. D. Deegan, *Phys. Rev. Lett.* **99**, 144501 (2007).  
 [11] S. Daniel and M. K. Chaudhury, *Langmuir* **18**, 3404 (2002).  
 [12] S. Daniel, S. Sircar, J. Gliem, and M. K. Chaudhury, *Langmuir* **20**, 4085 (2004).  
 [13] X. Noblin, R. Kofman, and F. Celestini, *Phys. Rev. Lett.* **102**, 194504 (2009).  
 [14] E. Benilov (2009), personal communication.  
 [15] S. Daniel, M. K. Chaudhury, and P.-G. de Gennes, *Langmuir* **21**, 4240 (2005).  
 [16] H. Lamb, *Hydrodynamics* (Cambridge University Press, Cambridge, England, 1932).  
 [17] M. Strani and F. Sabetta, *J. Fluid Mech.* **141**, 233 (1984).  
 [18] F. Celestini and R. Kofman, *Phys. Rev. E* **73**, 041602 (2006).  
 [19] D. V. Lyubimov, T. P. Lyubimova, and S. V. Shklyaev, *Phys. Fluids* **18**, 012101 (2006).  
 [20] X. Noblin, A. Buguin, and F. Brochard-Wyart, *Eur. Phys. J. E* **14**, 395 (2004).  
 [21] U. Thiele, J. M. Vega, and E. Knobloch, *J. Fluid Mech.* **546**, 61 (2006).  
 [22] A. Oron, S. H. Davis, and S. G. Bankoff, *Rev. Mod. Phys.* **69**, 931 (1997).  
 [23] S. Kalliadasis and U. Thiele, eds., *Thin Films of Soft Matter* (Springer, Wien, 2007), ISBN 978-3-211-69807-5.  
 [24] P.-G. de Gennes, *Rev. Mod. Phys.* **57**, 827 (1985).  
 [25] L. M. Pismen, *Phys. Rev. E* **64**, 021603 (2001).  
 [26] E. Doedel, H. B. Keller, and J. P. Kernevez, *Int. J. Bif. Chaos* **1**, 493 (1991).  
 [27] E. Doedel, H. B. Keller, and J. P. Kernevez, *Int. J. Bif. Chaos* **1**, 745 (1991).  
 [28] U. Thiele, K. Neuffer, M. Bestehorn, Y. Pomeau, and M. G. Velarde, *Colloid Surf. A* **206**, 87 (2002).  
 [29] S. Savel'ev, F. Marchesoni, and F. Nori, *Phys. Rev. E* **70**, 061107 (2004).